



HAL
open science

Discrimination of isomeric trisaccharides and their relative quantification in honeys using trapped ion mobility spectrometry

Cédric Przybylski, Véronique Bonnet

► To cite this version:

Cédric Przybylski, Véronique Bonnet. Discrimination of isomeric trisaccharides and their relative quantification in honeys using trapped ion mobility spectrometry. *Food Chemistry*, 2021, 341, pp.128182. 10.1016/j.foodchem.2020.128182. hal-03146652

HAL Id: hal-03146652

<https://hal.sorbonne-universite.fr/hal-03146652v1>

Submitted on 19 Feb 2021

HAL is a multi-disciplinary open access archive for the deposit and dissemination of scientific research documents, whether they are published or not. The documents may come from teaching and research institutions in France or abroad, or from public or private research centers.

L'archive ouverte pluridisciplinaire **HAL**, est destinée au dépôt et à la diffusion de documents scientifiques de niveau recherche, publiés ou non, émanant des établissements d'enseignement et de recherche français ou étrangers, des laboratoires publics ou privés.

1 **Discrimination of isomeric trisaccharides and their relative**
2 **quantification in honeys using Trapped Ion Mobility Spec-**
3 **trometry**

4 Cédric Przybylski*[†] and Véronique Bonnet[‡]

5 [†] Sorbonne Université, CNRS, Institut Parisien de Chimie Moléculaire, IPCM, 4 Place Jussieu,
6 75005 Paris, France.

7 E-mail: cedric.przybylski@sorbonne-universite.fr

8
9 [‡] Université de Picardie Jules Verne, Laboratoire de Glycochimie, des Antimicrobiens et des
10 Agroressources, LG2A, CNRS UMR 7378, 33 rue Saint Leu, 80039 Amiens, France.

11
12
13

14 **ABSTRACT**

15 Carbohydrates play a myriad of critical roles as key intermediaries for energy storage, cell wall
16 constituents, or also fuel for organisms. The deciphering of multiple structural isomers based on
17 the monosaccharides composition (stereoisomers), the type of glycosidic linkages (connectivity)
18 and the anomeric configuration (α and β), remains a major analytical challenging task. The pos-
19 sibility to discriminate 13 underivatized isomeric trisaccharides were reported using electrospray
20 ionization coupled to trapped ion mobility spectrometry (ESI-TIMS). After optimization of scan
21 ratio enhancing both the mobility resolving power (R) and resolution (r), fingerprints from 5 dif-
22 ferent honeys were obtained. Seven trisaccharides with relative content varying from 1.5 to
23 58.3%, were identified. It was demonstrated that their relative content and/or their ratio could be
24 used to ascertain origin of the honeys. Moreover, such direct approach constitutes an alternative
25 tool to current longer chromatographic runs, paving the way to a transfer as suitable routine
26 analysis.

27

28 Keywords (6 max): ion-mobility, carbohydrates, trisaccharides, honey, ESI-TIMS, collision cross
29 section.

30

31 1. INTRODUCTION

32 Carbohydrates or glycans are ubiquitous and the most abundant biological polymers in nature
33 occurring in many important biological processes (Varki, 2015). Their role and function are be-
34 yond key biological intermediary for energy storage and fuel for organisms. Indeed, they can, for
35 example, serve as building blocks for synthesis of higher macromolecules (nucleotides, glyco-
36 proteins, ...) or by modulating the molecular recognition in many physio-pathological processes
37 (Marth, 2008; Varki, 2015). Moreover, they are also the most rapidly evolving class of bio-
38 molecules through the evolution. Although it motivates numerous efforts for their characteriza-
39 tion, their structural deciphering remains a critical bottleneck. Indeed, carbohydrates sequencing
40 poses a major analytical challenge due to their inherent structural diversity, which is subject to a
41 pressing need emphasized by national research councils (EGSF and IBCarb Network & Euro-
42 pean Science Foundation, 2014; National Research Council (US), 2012). Such complexity is
43 mainly due to:

- 44 i) monosaccharides composition i.e. the carbohydrate based building blocks which are often
45 stereoisomers that differ only in their stereochemistry at one particular carbon atom (glucose
46 (Glc); galactose (Gal); mannose (Man)...).
- 47 ii) type of glycosidic linkages (connectivity) established between backbones of two building
48 blocks, leading to linear or branched structures with diverse regioisomers.
- 49 iii) anomeric configuration (α and β), relative to the stereogenic centre appearing consecutively
50 to a glycosidic bond formation. As example, considering a sequence of three monomers, more
51 than 1.13×10^7 trisaccharides can be theoretically obtained (Laine, 1994). Historically, NMR is
52 the reference method to determine the configurational information of carbohydrates, but require
53 mg scale amounts, and allows only relative detection limit of $\approx 3-5\%$, restricting the identification

54 of small amounts of coexisting isomers (Duus et al., 2000). Mass spectrometry (MS) is also very
55 used to identify and elucidate carbohydrates sequence, since it accurately and rapidly measure a
56 mass-to-charge ratio (m/z), with sub- μ g requirement, but intrinsic limit arising for stereoisomers
57 discrimination ability (Dell & Morris, 2001). Further information can be also extracted regarding
58 connectivity and so on sequence can be obtained using MS and iterative fragmentation (Ashline
59 et al., 2007; Carroll et al., 1995; Riggs et al., 2018; Schindler et al., 2017). Nevertheless, as re-
60 gards isomers, most of time very similar fragmentation pathways are obtained, impairing rigor-
61 ous discrimination. Liquid chromatography (LC) with or without coupling to MS represents an
62 alternative way for configurational isomers differentiation, but can be restricted by resolving
63 power to track one given isomer within potential others in complex mixture (Lareau et al., 2015).
64 In addition, derivatization step is very often a mandatory condition (Hofmann et al., 2015; Hof-
65 mann & Pagel, 2017). Recent IR or UV spectroscopies coupled to MS have proved their useful-
66 ness to obtain fingerprinting and delineate some anomeric forms (Ben Faleh et al., 2019; Mucha
67 et al., 2017; Riggs et al., 2018; Schindler et al., 2018; Gray et al., 2017). A promising approach
68 named ion mobility-MS (IM-MS) has been recently introduced and could overcome aforemen-
69 tioned limitations. IM-MS is a 2D method, which has potentiality to resolve glycan isomers
70 (Clowers et al., 2005; Hofmann & Pagel, 2017; Zheng et al., 2017). Practically, their correspond-
71 ing ions are separated not only according to their m/z , but also as function of their size and shape
72 in the gas phase, thanks to the conversion of mobility into a collision cross section (CCS). IM-
73 MS has been successfully applied to the characterization of large variety of derivatized or un-
74 derivatized carbohydrates using travelling wave ion mobility (TWIM) (Harvey et al., 2018;
75 Clowers et al., 2005; Paglia et al., 2014). Hofmann et al. (2015) have elegantly demonstrated that
76 six pentylaminated disaccharides can be differentiated according to their stereochemistry, con-

77 nectivity and anomeric configuration, but also that a relative anomeric content can be estimated
78 until 0.1%. Other IM technologies such as field asymmetric ion mobility spectrometry (FAIMS)
79 or drift tube ion mobility spectrometry (DTIMS) was also investigated for glycan analysis
80 (Gabryelski & Froese, 2003; Clowers et al., 2005; Gaye et al., 2015; Paglia et al., 2014; Xie et
81 al., 2020). Nonetheless, resolution of isomeric glycans by IM sometimes still fails to address
82 particular cases. Hence, the quest of improving IM separation efficiency remains one of the most
83 challenging field in IM-MS glycan analysis. To fulfil this objective, different strategies have
84 been deployed such as screening of various metal adduction (Huang & Dodds, 2013, 2015; Xie
85 et al., 2020; Zheng, Zhang, et al., 2017), or the formation of diastereomeric adducts (Gaye et al.,
86 2016) or the development of more resolving instruments. In this sense, Nagy et al. (2018) have
87 tailored serpentine ion pathway, and McKenna et al. (2019) have developed a cyclic TWIM al-
88 lowing multipass separations. Recently, trapped ion mobility spectrometry (TIMS) was intro-
89 duced by Bruker. TIMS was notably successfully applied for the analysis of glycosaminoglycan
90 (Wei et al., 2019) as well as to permethylated lacto-*N*-tetrasaccharides (Pu et al., 2016). In the
91 present work, we report efforts to discriminate 13 isomeric trisaccharides (Figure S1) without
92 any derivatization using electrospray ionization-TIMS (ESI-TIMS). The ability of the newly
93 TimsTOF™ instrument to differentiate studied carbohydrates according to their structures and
94 shapes was investigated. Moreover, usefulness of approach was validated as regards some crite-
95 ria such as an unambiguous identification, rapid analysis, relative quantification features of
96 trisaccharides in five honeys. We therefore propose the use of our TIMS strategy to extract gly-
97 can distribution to serve as characteristic fingerprint applicable in several field such as foodstuff
98 samples quality control, which remains a major challenge.

99 **2. MATERIALS AND METHODS**

100

101 **2.1. Standard Trisaccharides.** D-celotriose ($\geq 95\%$) and inulotriose ($\geq 90\%$), was purchased
102 from Megazyme (Berkshire, UK). Erllose ($\geq 95\%$), laminaritriose ($\geq 95\%$), D-gentianose ($\geq 97\%$),
103 1,4- β - D-mannotriose ($\geq 95\%$) and 4'galactosyllactose ($\geq 95\%$) were purchased from Carbosynth
104 (Berkshire, UK). Maltotriose hydrate ($\geq 95\%$), isomaltotriose ($\geq 98\%$), D-panose ($\geq 97\%$), D-(+)-
105 melezitose monohydrate ($\geq 99.0\%$), D-(+)-raffinose pentahydrate ($\geq 98.0\%$), 1-kestose ($\geq 98.0\%$)
106 were purchased from Sigma Aldrich (Saint-Quentin Fallavier, France).

107 **2.2 Solvents.** Methanol used for sample preparation was of LC grade and was purchased from
108 VWR (West Chester, PA, USA). Water was of ultrapure quality.

109 **2.3 Samples**

110 **2.3.1 Solutions.** Stock solutions were made at 10 mM in water and then diluted to 10 μ M in
111 methanol/water (1:1 v/v).

112 **2.3.2 Honeys.** 5 different honeys (3 from artisanal origin i.e. french lavender, rosemary and aca-
113 cia acquired directly from beekeepers and 2 from industrial source i.e. forest, eucalyptus).

114 All honeys are purchased from different regions of France such as Provence (french lavender and
115 rosemary), Alpine region (acacia), Auvergne region (forest) and Vosges mountains (eucalyptus).

116 Samples were prepared at 2% (w/v) in methanol/water (1:1 v/v), then further diluted by 1:2000
117 in the same solvent and passed through a 0.22 μ m filter to remove particulate matter, homoge-
118 nized by mechanical stirring and transferred to vials.

119 **2.4 GC-MS analyses.** Carbohydrate content in honey was controlled using the method described
120 by Sanz *et al.* (Sanz, M.L., Sanz, J., & Martínez-Castro, I. (2004). See Supporting Information
121 for further details.

122 **2.5 TimsTOF™ Experiments.** We used ESI-timsTOF™ (Bruker, Billerica, MA) operating with
 123 oTOF control v5.0 software. The source temperature was hold at 200°C, and the drying and
 124 nebulizing gas (N₂) operate at a flow rate of 3 L. min⁻¹ and at a pressure of 0.3 bar, respectively.
 125 The instrument was calibrated using Tuning Mix G24221 (Agilent Technologies, Les Ulis,
 126 France). Applied voltages were +4 kV and -0.5 kV for capillary and endplate offset, respectively.
 127 Acquisition was achieved in the *m/z* 50-3000 range with a center at *m/z* 200. TIMS separation
 128 depends on the gas flow velocity (*v_g*), elution voltage (*V_{elution}*), ramp time (*t_{ramp}*), base voltage
 129 (*V_{out}*) and the electric field (\vec{E}). The reduced mobility, *K₀*, can be calculated as follows :

$$130 \quad K_0 = \frac{v_g}{\vec{E}} = \frac{A}{(V_{elution} - V_{out})} \quad (\text{Eq. 1})$$

131 The mobility calibration constant *A* was determined using known reduced mobilities of tuning
 132 mix components. The resolving power (*R*) and resolution (*r*) are defined as $R = (1/K_0)/w$ and
 133 $r = 1.18 \times [(1/K_0)_2 - (1/K_0)_1]/(w_1 + w_2)$, where *w* is the full peak width at half-maximum.
 134 To improve separation efficiency, scan rate ($Sr = \Delta V_{ramp}/t_{ramp}$) was tuned thank to imeX™
 135 technology. For this, *t_{ramp}* is automatically set as function of manually adjusted ΔV_{ramp} . N₂ was
 136 used as buffer gas at funnel temperature (T = 305 K) with *v_g* set by the pressure difference of
 137 0.169 mbar. A potential of 350 Vpp was applied to radially confine the trapped ion cloud. The
 138 measured inverse reduced mobilities were converted into collision cross sections (CCS) using the
 139 Mason-Schamp equation:

$$140 \quad \Omega = \frac{(18\pi)^{1/2}}{16} \times \frac{q}{(k_B \times T)^{1/2}} \times \left[\frac{1}{m_i} + \frac{1}{m_g} \right]^{1/2} \times \frac{1}{N} \times \frac{1}{K_0} \quad (\text{Eq. 2})$$

141 where q is the ion charge, k_B is the Boltzmann constant, N is the gas number density, m_i is the
142 ion mass, and m_g is the gas molecule mass. TIMS-MS spectra and mobilograms were analyzed
143 using Compass Data Analysis 5.1 (Bruker).

144 **2.6 ESI-TIMS-MS analysis of the trisaccharides.**

145 Throughout this study, isomeric trisaccharides were analysed in the positive ion mode as singly
146 charged ions without any salt doping at m/z 505.176, 522.203, 527.158 and 543.132 for proton,
147 ammonium, sodium and potassium adducts, respectively. Separation occurred according to their
148 mobility. All samples was continuously infused at $5 \mu\text{L}\cdot\text{min}^{-1}$ via a 250 mL syringe.

149 **2.7 Theoretical Collision Cross Section Calculations.**

150 All initial geometry relaxations were performed using the Merck molecular force field
151 (MMFF94) implemented in Avogadro (v1.2). Geometry optimization was finalized using density
152 functional theory (DFT) calculations with NWChem (v7.0). Theoretical CCS calculations were
153 carried out in IMoS (v.1.1) using the average of ten trajectory method processes (Larriba & Ho-
154 gan, 2013).

155 **2.8 Data analysis.**

156 Statistical tests and Principal component analysis (PCA) were performed using Origin Pro 2016
157 (OriginLab Corporation, MA, USA.)

158 **3. RESULTS AND DISCUSSION**

159 **3.1 Ion mobility and collision cross sections determination of the library of trisaccharides.**

160 As observed elsewhere the type of adducts exhibits different dependencies upon the identity of
161 the bound cation, influencing the measured ion mobility (Huang & Dodds, 2013, 2015; Zheng,
162 Zhang, et al., 2017). Nevertheless, for a given trisaccharide, the ion mobility did not necessarily
163 increase/decrease proportionally according to the protonated form or ionic radii of the alkali

164 metal adduct as 154 pm, 99 pm, 137 pm and 151 pm for Na⁺, K⁺ and NH₄⁺, respectively. Most
165 importantly, it clearly appeared that the size of the adduct was not the only factor affecting the
166 ion mobility, since it can be hypothesised that each carbohydrate can adopt a preferred -most
167 stable- conformation, which can be either close or distinct according to a given cation. As re-
168 ported in Table 1, type of adduct can affect results at two level: (i) By supporting a straightfor-
169 ward identification. The mobility of two trisaccharide isomers, e.g. isomaltoriose and raffinose,
170 cannot be discriminated using protonated forms (both with $1/K_0 = 1.000 \text{ V.s/cm}^2$) but unambigu-
171 ously distinguished via ammoniated ($1/K_0 = 1.034$ versus 1.001 V.s/cm^2 , respectively), sodiated
172 ($1/K_0 = 1.033/0.984$ versus 1.020 V.s/cm^2 , respectively), or potassied adduct ($1/K_0 = 1.040/0.988$
173 versus 1.027 V.s/cm^2 , respectively). In this case, an increase in the size of the alkali metal ion
174 allowed the two isomers to assume conformations which were more readily distinguished by
175 mobility. (ii) By revealing other potential forms of trisaccharide such as epimers, connectivity
176 isomers or more simply other conformations due to distinct adduction sites. The mobility of two
177 forms for a given trisaccharide, e.g. sodiated and potassied 4'galactosyllactose yields to one and
178 two peaks detected by ion mobility ($1/K_0 = 0.990$ versus 1.006 and 1.018 V.s/cm^2 , respectively).
179 Moreover, after thorough examination of the various values summarized in table 1, and except
180 potential traces of maltotriose in isomaltoriose sample, as revealed by potassium adduct ($1/K_0 =$
181 1.041 versus 1.040 V.s/cm^2 , respectively), none standard trisaccharide seems to contain residual
182 presence of other one investigated in the herein study. One of the most emblematic features of
183 ion mobility hold in its ability to discriminate isomeric forms even with subtle variation. To ex-
184 plore the potential of timsTOF™ as regards such aforementioned aim, results on four trisaccha-
185 rides namely maltotriose,

186
187
188

Table 1. Recapitulative of the inverse reduced mobility of the 13 studied trisaccharides under various adducted forms at a scan rate of 5.5 V/ms and deduced collision cross section.

Name	Adduct	1/K ₀ (V.s.cm ⁻²)	TIMS ^{MS} CCS _{N₂} (Å ²)	
			Experimental*	Theoretical
Maltotriose	H	1.000	205.8	205.9±3.7
	NH ₄	1.006	206.8	206.7±4.1
	Na	1.038	213.3	214.2±6.2
	K	1.052/1.041	216.0/213.8	216.4±4.8
Isomaltotriose	H	0.997	205.2	205.0±4.8
	NH ₄	1.034	212.6	212.6±2.8
	Na	1.033/0.984	212.3/202.1	212.8±4.8
	K	1.040/0.988	213.5/203.0	213.5±3.3
Raffinose	H	0.997	205.2	205.3±2.7
	NH ₄	1.001	206.1	206.4±3.8
	Na	1.020	209.5	210.6±5.6
	K	1.027	211.0	211.3±3.8
Melezitose	H	0.999	205.5	205.4±2.9
	NH ₄	1.003	206.3	206.2±4.2
	Na	0.982	201.8	202.4±3.2
	K	0.986	202.6	203.2±3.1
1-Kestose	H	0.995	204.7	204.6±3.9
	NH ₄	1.013	208.3	208.2±2.9
	Na	0.999	205.5	206.7±5.2
	K	1.009	207.1	207.5±4.5
Gentianose	H	1.003	206.3	206.5±4.7
	NH ₄	1.036	213.0	213.4±4.3
	Na	1.016/0.985	208.7/202.4	208.0±6.1
	K	1.030/1.004	211.6/206.2	211.3±2.4
Panose	H	0.995	204.7	204.6±4.4
	NH ₄	1.007	207.0	206.8±3.5
	Na	1.018/1.025/0.981	209.2/210.7/201.6	209.3±7.0
	K	1.005/1.032	206.3/211.9	206.5±3.9
Cellotriase	H	1.021/1.070	210.2/220.1	210.4±3.7
	NH ₄	1.042	214.1	214.3±3.3
	Na	1.041/1.023	213.9/210.2	213.7±5.9
	K	1.048	215.2	214.9±3.4
Laminatriose	H	1.021/1.073	210.1/220.7	210.1±4.2
	NH ₄	1.062	218.3	218.3±4.5
	Na	1.029	211.5	211.3±5.6
	K	1.043/0.982	214.1/201.7	214.0±3.4
Mannotriose	H	1.040	213.9	213.9±3.9
	NH ₄	1.039	213.6	213.5±3.8
	Na	1.028	211.4	212.0±5.2
	K	1.041	213.7	214.0±2.1
4'galactosyllactose	H	0.998/1.014	205.3/208.5	205.0±4.1
	NH ₄	0.995/1.014	204.6/208.7	204.7±4.6
	Na	0.990	203.5	203.7±6.2
	K	1.006/1.018	206.6/209.1	206.9±3.6
Inulotriose	H	1.053	216.7	216.8±2.8
	NH ₄	1.045	214.7	214.9±3.3
	Na	0.992	203.9	203.9±5.9
	K	0.986/1.004	202.6/206.3	202.9±3.2
Erllose	H	0.991	203.9	204.6±3.6
	NH ₄	0.990	203.4	203.8±3.6
	Na	1.007	206.9	208.4±5.1
	K	0.990	203.3	203.5±4.2

189 * Standard deviation was 0.4 Å².

190 isomaltotriose, cellotriose and mannotriose under the various adducts were compared. Such
191 choice was motivated by differences in: i) connectivity, with isomaltotriose/maltotriose (α -D-
192 Glc (1 \rightarrow 6)/ α -D-Glc (1 \rightarrow 4), ii) anomery, with maltotriose/cellotriose (α -D-Glc (1 \rightarrow 4)/(β - D-
193 Glc(1 \rightarrow 4)) and iii) composition, with cellotriose/ mannotriose (β -D-Glc (1 \rightarrow 4) *versus* β -D-Man
194 (1 \rightarrow 4)) (Figure 1). Examination of protonated forms shows that only a slight mobility difference
195 occurred between the linkage isomers (1 \rightarrow 6 versus 1 \rightarrow 4), with 0.997 V.s/cm² and 0.995 V.s/cm²
196 for isomaltotriose and maltotriose, respectively (Figure 1a brown and blue trace, respectively).
197 Varying α - to β - linkage, it reveals a significant shift from 0.995 V.s/cm² to 1.021 and 1.070
198 V.s/cm² for maltotriose to cellotriose, respectively (Figure 1a blue and green trace, respectively).
199 The detection of two peaks, with similar abundance for cellotriose, can be putatively ascribed to
200 either the presence of two equivalent protomers and/or to the co-existence of both α - and β -
201 anomers. Using a different fully compositional isomer, one exhibits also a different mobility
202 from 1.021/1.070 V.s/cm² to 1.040 V.s/cm² for cellotriose to mannotriose, respectively (Figure 1a
203 green and pink trace, respectively). In contrast to protonated forms, the ammoniated ones present
204 a better difference like for isomaltotriose/maltotriose couple with 1.034/1.006 V.s/cm² (Figure
205 1b, brown and blue trace, respectively), and for maltotriose/cellotriose one with 1.006/1.042
206 V.s/cm² (Figure 1b, blue and green trace, respectively). Mobility values were quasi similar for
207 cellotriose/mannotriose one with 1.042/1.039 V.s/cm² (Figure 1b, green and pink trace, respec-
208 tively) impairing any discrimination between us in such conditions. However, it was quoted out
209 that with ammonium, only one peak is detected for the four carbohydrates even for cellotriose
210 while two peaks were observed for protonated one. It seems to indicate that either only one am-
211 monium attachment site exists or that an absence of interconversion occurs during the course of

212 the experiment. Under sodiated forms, isomaltotriose shows two distinct peaks at 0.984 and
 213 1.033 V.s/cm² but differing

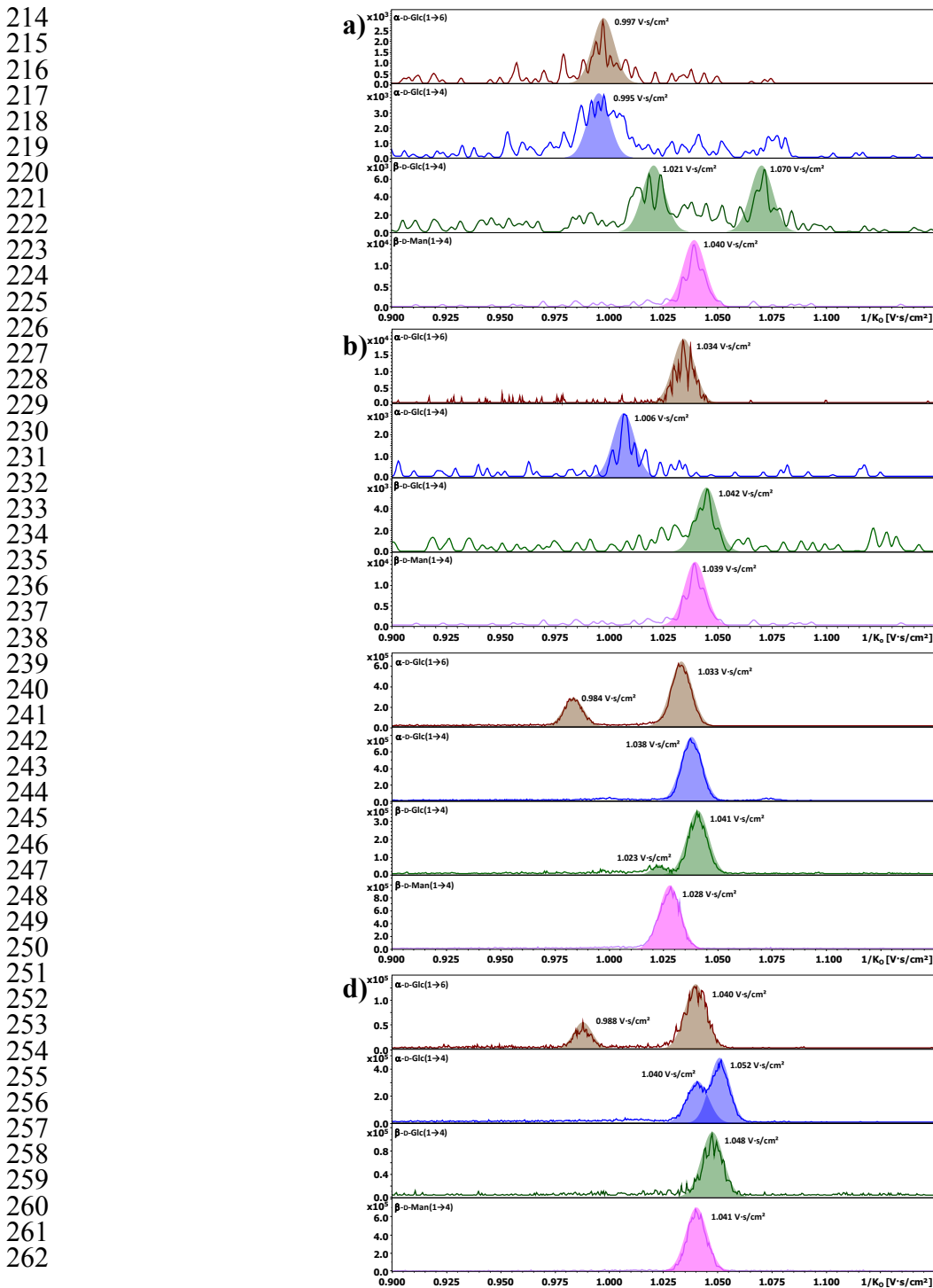


Figure 1. TIMS based mobilograms without any smoothing for trisaccharides showing difference in connectivity: α -D-Glc (1 \rightarrow 6) versus α -D-Glc (1 \rightarrow 4) (isomaltotriose versus maltotriose),

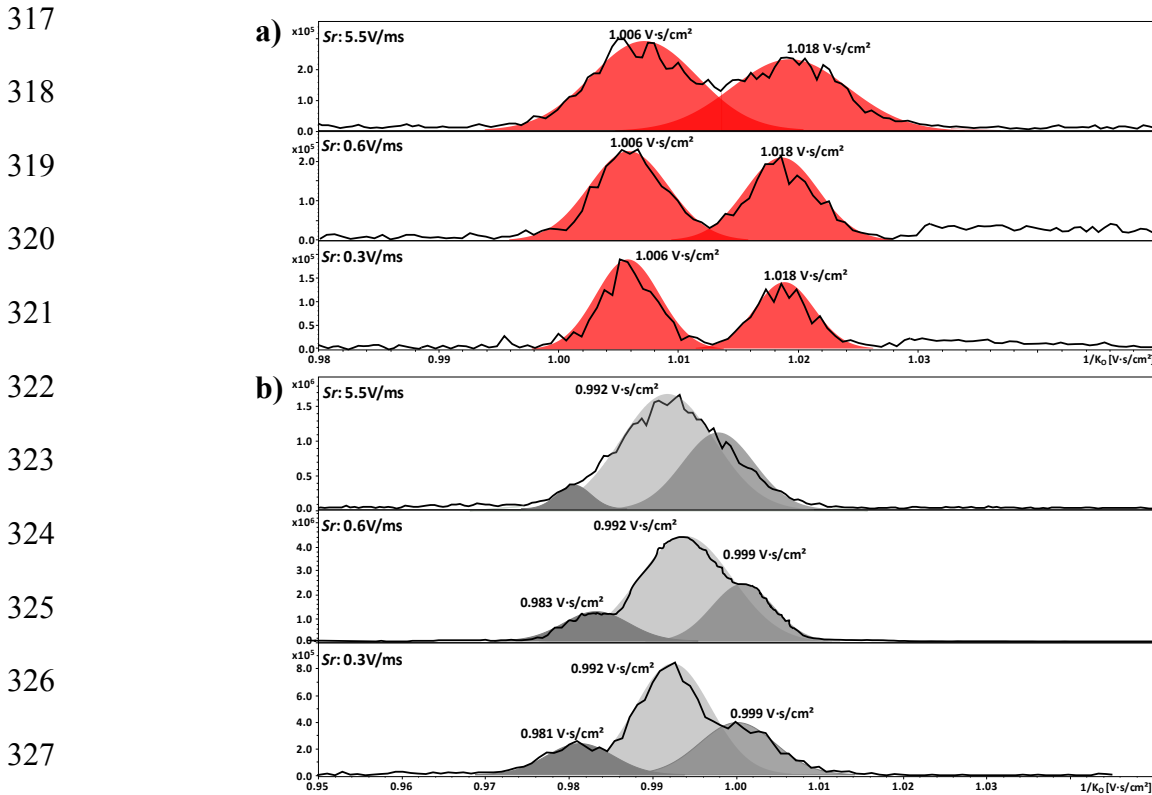
266 anomery ((α -D-Glc (1 \rightarrow 4) *versus* β -D-Glc (1 \rightarrow 4) (maltotriose *versus* cellotriose) and composi-
267 tion: β -D-Glc (1 \rightarrow 4) *versus* β -D-Man (1 \rightarrow 4) (cellotriose *versus* mannotriose) for a) singly proto-
268 nated, b) singly sodiated, c) singly ammoniated and d) singly potassied trisaccharides. Measure-
269 ment was achieved at a scan rate of 5.5 V/ms.
270 from the unique one recorded at 1.038 V.s/cm² for maltotriose (Figure 1c, brown and blue trace,
271 respectively). This last one is very close from its β - anomer, cellotriose, with a mobility at 1.041
272 V.s/cm² (Figure 1c, green trace). Moreover, as for protonated form, a second but lower peak was
273 detected at 1.023 V.s/cm². Sodiated mannotriose exhibits lower mobility shift (1.028 V.s/cm²,
274 Figure 1c, pink trace). Again with sodium, one can hypothesize that the observation of only one
275 mobility peak from maltotriose and mannotriose may be attributed to its inability to mutarotate,
276 and present two distinct α/β anomers at the OH group of C-1. The isomaltotriose and cellotriose
277 both displayed two mobility features, presumably due to its α/β mutarotation, while maltotriose
278 and mannotriose only displayed one such feature, perhaps due to the influence of the composi-
279 tion or linkage on mutarotation, and leading to a preference for only a single α or β anomer.
280 Nonetheless, at this stage, it cannot be completely excluded that the two mobility peaks observed
281 for isomaltotriose and cellotriose would result from different sodium attachment locations. As
282 regards potassied forms, similar behaviour than for sodiated ones were obtained but with higher
283 mobility values. However, two exceptions were highlighted for maltotriose and cellotriose. For
284 the former, two unresolved peaks were detected at 1.040 V.s/cm² and 1.052 V.s/cm² (Figure 1d,
285 blue trace) instead of only one with sodium (Figure 1c, blue trace). For the latter, only one peak
286 was detected at 1.048 V.s/cm² (Figure 1d, green trace), instead of two with sodium (Figure 1c,
287 green trace). Taking into account the results obtained for all trisaccharides (Table 1 and Figure
288 1), some general trends can be drawn where non-reducing trisaccharides (raffinose, melezitose,
289 1-kestose, gentianose, inulotriose, erlose) were higher in mobility, i.e. smaller in collision cross
290 section or more compact in nature than the reducing ones (maltotriose, isomaltotriose, panose,

291 celotriose, laminaritriose, mannotriose, 4'galactosyllactose). Additionally, the former exhibits
292 only one mobility peak, and thus as speculated above, we have reasonably attributed this obser-
293 vation to a 'locked' configuration at the anomeric carbon, while the latter i.e. their reducible
294 counterparts lead to two mobility peaks, potentially from α/β anomeric configurations as previ-
295 ously suggested (Nagy et al., 2018). However, it must keep in mind that the coexistence of mul-
296 tiple cation attachment sites or impurities at traces level can also exist and that may explain the
297 results of sodiated and potassied gentianose as well as potassied inulotriose. Moreover, for a
298 given monosaccharide composition, comparison of α versus β linked trisaccharides reveals that
299 the β linked was more elongated (higher inverse reduced mobility i.e. lower mobility) than the α -
300 linked (lower inverse reduced mobility i.e. higher mobility). In summary, TIMS experiments
301 achieved until now at a defined scan rate (Sr) of 5.5 V/ms, and taking into account the type of
302 adduct, compositional isomers, regioisomers and anomers, can be distinguished readily from
303 each other on the basis of their elution voltage converted to ion mobility values and calculated
304 CCS. Herein CSS values are in good agreement with some previously reported in literature (Ta-
305 ble S1).

306 **3.2 Enhancing isomers separations by adjusting ion mobility resolution.**

307 The diminishment of Sr , aiming to reduce/avoid excessive ion mobility peak overlapping, sig-
308 nificantly increases the mobility resolving power by ≈ 1.7 to 4 fold. As example, for singly
309 potassied 4'galactosyllactose, Sr adjusted from 5.5 V/ms to 0.6 V/ms followed by 0.3 V/ms as
310 the lowest scan value, led to high mobility resolving power ($R \sim 87/92, 150/153$ to $175/183$, re-
311 spectively) (Figure 2a). Even if the presence of two peaks issued from potassied
312 4'galactosyllactose was already distinguishable at $Sr = 5.5$ V/ms, lowering Sr offers a substantial
313 enhancement of mobility resolution leading to a partial and almost complete baseline resolution

314 with $r = 0.7, 1.0$ and 1.3 , respectively. Conversely, in the case of sodiated inulotriose only one
 315 large peak was initially detected. Varying Sr led to a significant increase of the mobility resolv-
 316 ing power as well as $R \sim 66, 133-170$ and $137-226$, for Sr 5.5, 0.6 and 0.3 V/ms, respectively.



328

329 **Figure 2.** TIMS based mobilograms showing the influence of the scan ratio (Sr) from 5.5 V/ms
 330 to 0.3V/ms on both the resolving power (R) and resolution (r) for a) singly potassiumated
 331 4'galactosyllactose and b) singly sodiated inulotriose.
 332

333 It has thus permitted to highlight the presence of three different forms (Figure 2b). Such en-
 334 hancement resulted in a possible mobility resolution $r = 0.5$ for peak 1/2 at $Sr = 0.6$ V/ms, which
 335 is slightly improved with $r = 0.7$ and 0.6 for peak 1/2 and 2/3, respectively, at $Sr = 0.3$ V/ms.
 336 However, it was quoted out that each diminishment of Sr yields also to a slightly and gradual
 337 loss of sensitivity.

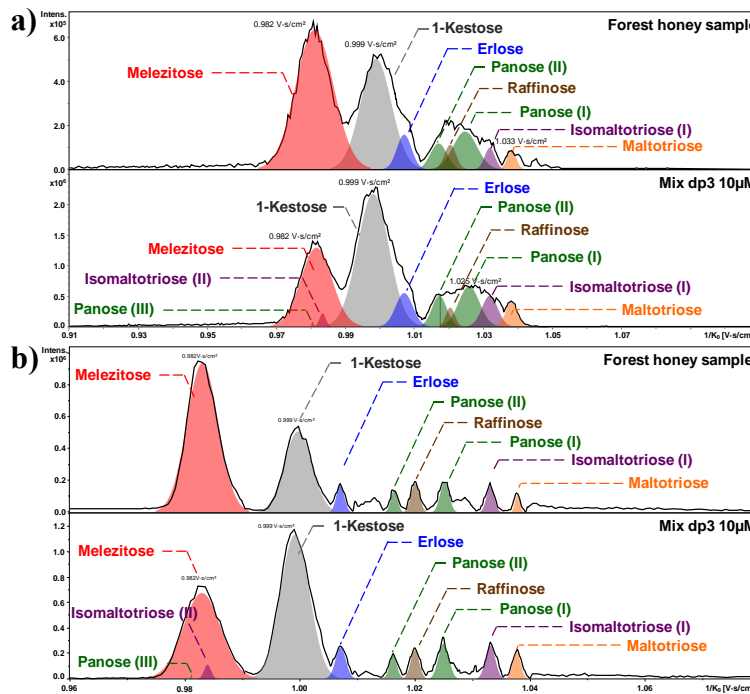
338

339 **3.4 Identification and estimation of relative trisaccharides content in honeys.**

340 Nowadays, traceability of foodstuff is of prime importance to ensure the highest level of con-
341 sumer protection. Products must fulfil the criteria of quality that, day by day, are becoming more
342 and more specific and exigent. Implemented detection and quantification methods are mainly
343 based on chromatography. They are continuously improved to address the more and more restric-
344 tive quality rules of food industry, requiring the highest sensitivity. Such analytical methods
345 should afford to reveal the conformity of the products, especially as regards possible contamina-
346 tion or adulteration, which can be hazardous to health or bias the real nutritional value. Honey is
347 one of the most complex mixture of carbohydrates produced in nature and represents a good ex-
348 ample since it is subject to these same demands. Literature reports that carbohydrate content of
349 natural honey is mainly composed of monosaccharides (essentially glucose and fructose), disac-
350 charides and trisaccharides at a level of 50-70%, 15-35% and 2-10%, respectively (Sanz et al.,
351 2005). Presence of several oligosaccharides, portray only minority of the whole carbohydrates
352 content, but can constitute a fingerprint indexing the honey authenticity and floral origin. Fur-
353 thermore, examination of literature showed that if mono- and disaccharides content are the
354 mainly studied carbohydrates during honeys analysis, trisaccharides have potential to be finer
355 discriminating factor (Kaškonienė, V. & Venskutonis, P. R. 2010). Our TIMS approach was ap-
356 plied to reveal, identify and gain relative content of trisaccharides in honeys. As example, a for-
357 est based honey was infused and analysed by TIMS using a Sr of 0.6 V/ms. Resulting mobilo-
358 gram showed two intense partially resolved peaks at $1/K_0 = 0.982$ and 0.999 V.s/cm² and one
359 with a lower abundance but with a very large mobility range distribution, mainly unresolved,
360 centred around 1.025 V.s/cm² (Figure 3a, top mobilogram). It can be also quoted out that the
361 mobility range from 0.965 to 1.055 V.s/cm², ascribed to all detected peaks from honey, can theo-

362 retically correspond to twelve among the thirteen studied trisaccharides herein. A comparative
 363 GC-MS analysis was achieved, where 7 trisaccharides were identified among them i.e. raffinose,
 364 1-kestose, erlose, melezitose, maltotriose, panose and isomaltotriose (Figure S2). A mixture con-
 365 taining these seven standard trisaccharides at 10 μ M (Mix dp3, see experimental section) was
 366 prepared. The mobilogram of Mixdp3 unambiguously confirms the presence of melezitose and
 367 1-kestose ascribed to the two predominant peaks observed by ion mobility. Erlose can also be
 368 extracted from

369
 370
 371
 372
 373
 374
 375
 376
 377
 378
 379
 380
 381
 382
 383
 384
 385
 386
 387
 388
 389
 390
 391
 392
 393
 394



395 **Figure 3.** TIMS based mobilogram of the various singly sodiated trisaccharides ions of both
 396 standard mixture (top) and forest honey (below) acquired with the scan ratio of a) 0.6 V/ms and
 397 b) 0.3 V/ms.

399 the abnormal peak tailing of 1-Kestose peak. The deconvolution of the large mobility distribution
 400 in the 1.012-1.042 V.s/cm² range allows the putative assignment of panose, raffinose, isomalto-
 401 triose and maltotriose (Figure 3a, below mobilogram). For melezitose, 1-kestose/erlose and mal-
 402 totriose, the resolving power (*R*) is 84, 69 and 201, respectively, while the unresolved peak of the

403 set constituted of panose, raffinose and isomaltotriose is only 54. As regards resolution (r), val-
404 ues of 0.77, 0.80 and 0.77 for melezitose to 1-kestose/erlose, 1-kestose/erlose to unresolved set
405 and unresolved set to maltotriose, respectively, were obtained. Nonetheless, it appears clearly
406 that a complete mobility resolution is a mandatory condition to fully address the unambiguous
407 and straightforward identification of the carbohydrates in crude samples. To reach that, a Sr of
408 0.3 V/ms was applied leading to a substantial improvement of both resolving power and mobility
409 resolution with a close baseline resolution for every compounds (Figure 3b). Specifically, with
410 such settings, erlose trace can be easily discriminated from 1-kestose, as well as the full set of
411 panose, raffinose, isomaltotriose and maltotriose. Using lower scan rates yields to clear im-
412 provement in both R and r with all values included in the range 126-722 and 1.15-2.19, respec-
413 tively. It contrasts with results obtained elsewhere as raffinose, isomaltotriose, melezitose and
414 maltotriose were not separated under $[M+Na]^+$ and were hardly resolved with a maximal $r =$
415 0.25, 0.52, 1.42, 0.27, 1.15 and 0.87 for maltotriose-isomaltotriose, maltotriose-raffinose, malto-
416 triose-melezitose, isomaltotriose-raffinose, isomaltotriose-melezitose and raffinose-melezitose
417 couple, respectively (Xie et al., 2020). Our GC-MS analysis showed similar profile to those pre-
418 viously observed by Sanz et al. (Sanz, M.L., Sanz, J., & Martínez-Castro, I. (2004) and de la
419 Fuente et al. (2011) as regards elution order and observation of possible Z and E isomers for mal-
420 totriose, isomaltotriose and panose (Figure S2). Nonetheless, several peaks for aforementioned
421 trisaccharides are also systematically observed without any derivatization (Figure 3 and Table 1).
422 Such results suggest that configurational isomers pre-exist before derivatization due to α/β mu-
423 tarotation, as evocated in section 3.1. Moreover, our TIMS approach overcomes frequent co-
424 elution problems observed with non-polar GC columns, especially between raffinose and kesto-
425 ses that may lead to misestimation (Sanz, M.L., Sanz, J., & Martínez-Castro, I., 2004; Ruiz-

426 Matute et al., 2010; de la Fuente et al., 2011). All R and r metrics are listed in Table S2. Interest-
427 ingly, beyond only qualitative determination (identification criterion), one can access to a rela-
428 tive quantification (relative content criterion), providing to take into account the variation in re-
429 sponse factor due to various ionization efficiency by comparing signals from independent analy-
430 sis of the molecules alone or in mixture. Therefore, area integration allows establishing the rela-
431 tive content of the honeys as regards the seven trisaccharides. In this sense, TIMS approach re-
432 veals a similar abundance order both with $Sr = 0.6$ and 0.3 V/ms as follows: melezitose (28.2-
433 28.3%) > raffinose (20.8-21.4%) > panose (13.7%) > erlose (12.2-12.6%) > 1-kestose (10.5-
434 10.8%) > maltotriose (8.4-8.5%) > isomaltotriose (5.1-5.7%). Such content matched very well
435 with those obtained by GC-MS analysis (Table 2). Both nature and relative abundance of trisac-
436 charides can represent a potential signature of the floral sources (Cotte et al., 2003; Kaškonienė
437 & Venskutonis, 2010). The data obtained for the seven carbohydrates and from the five honeys
438 (Table S3) were analyzed in a one-way ANOVA. Results ported that all overall ANOVA p -value
439 are smaller than 0.05 (95% confidence interval), hence at least two of the five honey have sig-
440 nificantly different means whatever the given trisaccharides. Further statistical treatment by us-
441 ing Tukey test, i.e. mean comparisons, reveals further information regarding relationships be-
442 tween honeys (Table S4 and Figure S3).

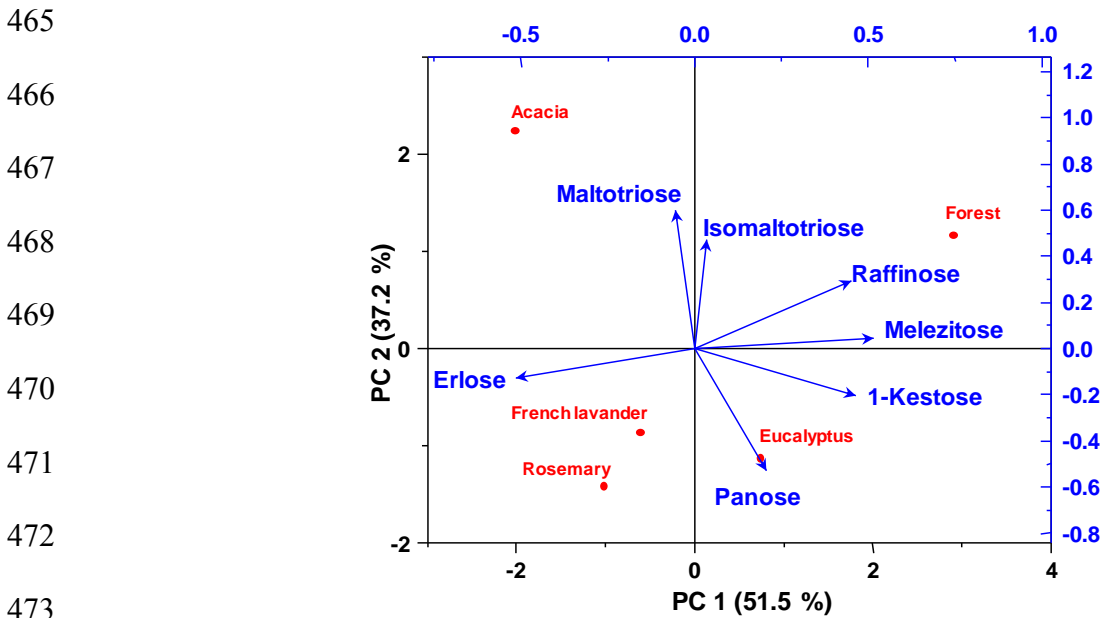
443
444

445 **Table 2.** Relative content of the seven positively identified trisaccharides according to both the
 446 two-based TIMS scan ratio (*Sr*) and GC-MS for the forest honey.

Identified trisaccharides	Relative content (%) (n=10)		
	<i>Sr</i> setting		GC-MS
	0.6 V/ms	0.3 V/ms	
1-Kestose	10.8 ± 1.4	10.5 ± 1.6	10.6 ± 2.3
Erlose	12.2 ± 0.5	12.6 ± 0.5	12.4 ± 1.5
Isomaltotriose	5.1 ± 0.7	5.7 ± 0.5	5.5 ± 1.2
Maltotriose	8.5 ± 0.5	8.4 ± 0.5	8.1 ± 1.4
Melezitose	28.2 ± 2.4	28.5 ± 2.1	28.7 ± 2.6
Panose	13.7 ± 1.5	13.7 ± 1.6	13.6 ± 1.8
Raffinose	21.4 ± 2.1	20.6 ± 1.8	20.9 ± 2.3

447
 448
 449 All of honey seemed to be discriminated using at least two significant trisaccharides content. In
 450 addition, it appears that all the targeted trisaccharides can be used to the distinction of acacia and
 451 forest honeys on one hand and rosemary and forest honeys on the other hand. All the seven
 452 trisaccharides regarding their more or less complementary balances of significant/non-significant
 453 means as 2/8 (1-kestose, isomaltotriose, panose, raffinose), 3/7 (erlose) and 1/9 (maltotriose,
 454 melezitose) could be chosen as a relevant role authenticity/floral marker. Standardized principal
 455 component analysis can explain the 88.7% of total variance using the two first components,
 456 reaching 100% through four first components. It can be observed that the first principal compo-
 457 nent is mainly a function of melezitose and erlose. The second principal component is essentially
 458 a function of maltotriose and panose (Figure 4). In summary, the most important relative weights
 459 in the first component are both positive (melezitose) and negative (erlose), this may be inter-
 460 preted as a general balance to serve as index of each honey. A similar behaviour was obtained for
 461 the second component where weights are both positive (maltotriose) and negative (panose). Su-
 462 perimposition of the botanical origins represented according to the two first components, leading

463 to the botanical origin coordinates, known as centroid, using the scores obtained for honeys
464 against their botanical origin.



474 **Figure 4.** Superimposition of the representation of carbohydrates (blue) and of botanical origins
475 (red) as a function of the two first principal components.
476

477 It may be seen that forest honey obtains the highest scores for the first component, while acacia
478 and rosemary obtain the lowest. As such, the group of trisaccharides formed by melezitose, raffi-
479 nose and erlose may play an important role in distinguishing among honeys of different botanical
480 origins as observed in another study (Cotte et al. 2004). Acacia honey obtains higher scores in
481 the second principal component than the remainder of botanical origins, above all relative to for-
482 est and much more to rosemary, eucalyptus and french lavender. Based on the two first principal
483 components analysis and Tukey test, taking into account that all seven trisaccharides were de-
484 tected in the five honeys, we can suggest to use both abundance and ratio of trisaccharide as dis-
485 criminant factor. For example, the herein honeys can be characterized with carbohydrates bal-
486 ance: forest with $\geq 20\%$ of melezitose and $\geq 20\%$ of melezitose/raffinose > 1 ; acacia with malto-

487 triose >10%, panose <10% and erlose/maltotriose >4.5%; eucalyptus with panose >15%; 1-
488 kestose >5% and panose /1-kestose >2%; french lavender with maltotriose >5%, panose >10%
489 and erlose/maltotriose > 9%; rosemary with maltotriose <5%, panose >10% and er-
490 lose/maltotriose >9.5%. Such factors given to depict possible discriminative tree, need to be used
491 with many precautions, since only a restricted set of honeys was assessed. Such approach should
492 be further enriched with both a larger panel of honeys and other potential but very rare trisaccha-
493 rides such as neo-kestose, 6-kestose, planteose or also theanderose. Another strategy holds in the
494 introduction of canonical discriminant (Nozal et al., 2005), as a potential key to achieve a
495 straightforward honeys classification, but the judicious choice of the suitable factor to consider-
496 ate remains a delicate approach. Indeed, if single factors as presence and/or abundance of trisac-
497 charides can be very effective to characterize the differences among monofloral honeys, that
498 could be a more daunting task with honeys generically classified as multifloral. Moreover, the
499 ratio between some mono-, di- or trisaccharides such as for example fructose/glucose, mal-
500 tose/isomaltose, sucrose/turanose, and maltose/turanose or also maltotriose/(raffinose + erlose +
501 melezitose) is another indicator that may be used to ascertain honey authenticity (Nozal et al.,
502 2005). For example, an acacia honey was distinguished by a high maltose/isomaltose ratio (11:1 to
503 25:9), while this ratio for linden and honeydew honeys was remarkably lower, 2.2 and 2.0-2.5,
504 respectively (Molnár-Perl & Horváth, 1997). A similar strategy was successfully used by Cotte et
505 al. (2003) regarding maltotriose/trisaccharides ratio to distinguish various lavender honey.

506 **4. CONCLUSIONS**

507 We demonstrate in this work that the fast and direct analysis by TIMS represents a powerful and
508 suitable alternative to longer chromatographic run, with analysis time of few minutes to more
509 than one hour, respectively, to distinguish between 13 isomeric trisaccharides. Our IM strategy

510 has been successfully applied to 5 honeys, which are traditionally classified by time-consuming
511 and high levels of expertise requiring pollen analyses. Our TIMS method tackles these aforemen-
512 tioned bottlenecks, by introducing an orthogonal strategy using 2 parameters i.e. m/z and CCS.
513 After both optimization of TIMS resolution and determination of response factor due to various
514 ionization efficiency, extraction of areas from IM afforded a straightforward relative quantifica-
515 tion of trisaccharides in the honeys. Then, principal component analysis has been successfully
516 employed as a first approach to characterize the 5 honeys, showing similarities or differences in
517 trisaccharide content aiming to delineate potential floral markers. Moreover, m/z and CCS could
518 be supplemented by upstream separation and MS/MS spectra to serve as additional dimensions.
519 Ongoing expanding of this approach to operate at middle to high throughput, with or without
520 other upstream separation methods, paves the way to the introduction of new routinely means in
521 the field of glycomics.

522 **ACKNOWLEDGMENTS**

523 This work was supported by CEA and the French Ministry of Research and National Research
524 Agency as part of the French metabolomics and fluxomics infrastructure (MetaboHUB, ANR-11-
525 INBS-0010 grant).

526 **REFERENCES**

- 527 Ashline, D. J., Lapadula, A. J., Liu, Y.-H., Lin, M., Grace, M., Pramanik, B., & Reinhold, V. N. (2007). Car-
528 bohydrate Structural Isomers Analyzed by Sequential Mass Spectrometry. *Analytical Chemistry*, 79,
529 3830- 3842. <https://doi.org/10.1021/ac062383a>.
- 530 Ben Faleh, A., Warnke, S., & Rizzo, T. R. (2019). Combining Ultrahigh-Resolution Ion-Mobility Spectrome-
531 try with Cryogenic Infrared Spectroscopy for the Analysis of Glycan Mixtures. *Analytical Chemistry*,
532 91, 4876- 4882. <https://doi.org/10.1021/acs.analchem.9b00659>.

533 Carroll, J. A., Willard, D., & Lebrilla, C. B. (1995). Energetics of cross-ring cleavages and their relevance to
534 the linkage determination of oligosaccharides. *Analytica Chimica Acta*, 307, 431- 447.
535 [https://doi.org/10.1016/0003-2670\(94\)00514-M](https://doi.org/10.1016/0003-2670(94)00514-M).

536 Clowers, B. H., Dwivedi, P., Steiner, W. E., Hill, H. H., & Bendiak, B. (2005). Separation of sodiated isobaric
537 disaccharides and trisaccharides using electrospray ionization-atmospheric pressure ion mobility-time
538 of flight mass spectrometry. *Journal of the American Society for Mass Spectrometry*, 16, 660- 669.
539 <https://doi.org/10.1016/j.jasms.2005.01.010>.

540 Cotte, J. F., Casabianca, H., Chardon, S., Lheritier, J., & Grenier-Loustalot, M. F. (2003). Application of car-
541 bohydrate analysis to verify honey authenticity. *Journal of Chromatography A*, 1021, 145- 155.
542 <https://doi.org/10.1016/j.chroma.2003.09.005>.

543 Cotte, J. F., Casabianca, H., Chardon, S., Lheritier, J., & Grenier-Loustalot, M. F. (2004). Chromatographic
544 analysis of sugars applied to the characterisation of monofloral honey. *Analytical and Bioanalytical*
545 *Chemistry*, 380, 698-705. <https://doi.org/10.1007/s00216-004-2764-1>. de la Fuente, E., Ruiz-Matute,
546 A.I., Valencia-Barrera, R.M., Sanz J., Martínez Castro I. (2011). Carbohydrate composition of Span-
547 ish unifloral honeys. *Food Chemistry*, 129, 1483–1489

548 Dell, A., & Morris, H. R. (2001). Glycoprotein Structure Determination by Mass Spectrometry. *Science*, 291,
549 2351. <https://doi.org/10.1126/science.1058890>.

550 Duus, J. Ø., Gotfredsen, C. H., & Bock, K. (2000). Carbohydrate Structural Determination by NMR Spectros-
551 copy: Modern Methods and Limitations. *Chemical Reviews*, 100, 4589- 4614.
552 <https://doi.org/10.1021/cr990302n>.

553 EGSF and IBCarb Network & European Science Foundation. (2014). *A Roadmap for Glycosciences in*
554 *Europe*. (Vol. 1- 1). EGSF and IBCarb Network & European Science Foundation. A Roadmap for
555 Glycosciences in Europe. [http://ibcarb.com/wp-content/uploads/A-roadmap-for-Glycoscience-in-](http://ibcarb.com/wp-content/uploads/A-roadmap-for-Glycoscience-in-Europe.pdf)
556 [Europe.pdf](http://ibcarb.com/wp-content/uploads/A-roadmap-for-Glycoscience-in-Europe.pdf). 2014. <http://ibcarb.com/wp-content/uploads/A-roadmap-for-Glycoscience-in-Europe.pdf>.

557 Gabryelski, W., & Froese, K. L. (2003). Rapid and sensitive differentiation of anomers, linkage, and position
558 isomers of disaccharides using High-Field Asymmetric Waveform Ion Mobility Spectrometry

559 (FAIMS). *Journal of The American Society for Mass Spectrometry*, 14, 265- 277.
560 [https://doi.org/10.1016/S1044-0305\(03\)00002-3](https://doi.org/10.1016/S1044-0305(03)00002-3).

561 Gaye, M. M., Kurulugama, R., & Clemmer, D. E. (2015). Investigating carbohydrate isomers by IMS-CID-
562 IMS-MS: precursor and fragment ion cross-sections. *Analyst*, 140, 6922- 6932.
563 <https://doi.org/10.1039/C5AN00840A>.

564 Gaye, M. M., Nagy, G., Clemmer, D. E., & Pohl, N. L. B. (2016). Multidimensional Analysis of 16 Glucose
565 Isomers by Ion Mobility Spectrometry. *Analytical Chemistry*, 88, 2335- 2344.
566 <https://doi.org/10.1021/acs.analchem.5b04280>.

567 Gray, C. J., Schindler, B., Migas, L. G., Pičmanová, M., Allouche, A. R., Green, A. P., Mandal, S., Motawia,
568 M. S., Sánchez-Pérez, R., Bjarnholt, N., Møller, B. L., Rijs, A. M., Barran, P. E., Compagnon, I., Ey-
569 ers, C. E., & Flitsch, S. L. (2017). Bottom-Up Elucidation of Glycosidic Bond Stereochemistry. *Ana-*
570 *lytical Chemistry*, 89, 4540- 4549. <https://doi.org/10.1021/acs.analchem.6b04998>.

571 Harvey, D. J., Seabright, G. E., Vasiljevic, S., Crispin, M., & Struwe, W. B. (2018). Isomer Information from
572 Ion Mobility Separation of High-Mannose Glycan Fragments. *Journal of the American Society for*
573 *Mass Spectrometry*, 29, 972- 988. <https://doi.org/10.1021/jasms.8b05810>.

574 Hofmann, J., Hahm, H. S., Seeberger, P. H., & Pagel, K. (2015). Identification of carbohydrate anomers using
575 ion mobility–mass spectrometry. *Nature*, 526, 241- 244. <https://doi.org/10.1038/nature15388>.

576 Hofmann, J., & Pagel, K. (2017). Glycan Analysis by Ion Mobility–Mass Spectrometry. *Angewandte Chemie*
577 *International Edition*, 56, 8342- 8349. <https://doi.org/10.1002/anie.201701309>.

578 Huang, Y., & Dodds, E. D. (2013). Ion Mobility Studies of Carbohydrates as Group I Adducts : Isomer Spe-
579 cific Collisional Cross Section Dependence on Metal Ion Radius. *Analytical Chemistry*, 85,
580 9728- 9735. <https://doi.org/10.1021/ac402133f>.

581 Huang, Y., & Dodds, E. D. (2015). Discrimination of Isomeric Carbohydrates as the Electron Transfer Prod-
582 ucts of Group II Cation Adducts by Ion Mobility Spectrometry and Tandem Mass Spectrometry. *Ana-*
583 *lytical Chemistry*, 87, 5664- 5668. <https://doi.org/10.1021/acs.analchem.5b00759>.

584 Kaškonienė, V., & Venskutonis, P. R. (2010). Floral Markers in Honey of Various Botanical and Geographic
585 Origins : A Review. *Comprehensive Reviews in Food Science and Food Safety*, 9, 620- 634.
586 <https://doi.org/10.1111/j.1541-4337.2010.00130.x>.

587 Laine, R. A. (1994). Invited Commentary : A calculation of all possible oligosaccharide isomers both branched
588 and linear yields 1.05×10^{12} structures for a reducing hexasaccharide : The Isomer Barrier to devel-
589 opment of single-method saccharide sequencing or synthesis systems. *Glycobiology*, 4, 759- 767.
590 <https://doi.org/10.1093/glycob/4.6.759>.

591 Lareau, N. M., May, J. C., & McLean, J. A. (2015). Non-derivatized glycan analysis by reverse phase liquid
592 chromatography and ion mobility-mass spectrometry. *Analyst*, 140, 3335- 3338.
593 <https://doi.org/10.1039/C5AN00152H>.

594 Larriba, C., & Hogan, C. J. (2013). Ion Mobilities in Diatomic Gases : Measurement versus Prediction with
595 Non-Specular Scattering Models. *The Journal of Physical Chemistry A*, 117, 3887- 3901.
596 <https://doi.org/10.1021/jp312432z>.

597 Marth, J. D. (2008). A unified vision of the building blocks of life. *Nature Cell Biology*, 10, 1015- 1015.
598 <https://doi.org/10.1038/ncb0908-1015>.

599 McKenna, K. R., Li, L., Baker, A. G., Ujma, J., Krishnamurthy, R., Liotta, C. L., & Fernández, F. M. (2019).
600 Carbohydrate isomer resolution via multi-site derivatization cyclic ion mobility-mass spectrometry.
601 *Analyst*, 144, 7220- 7226. <https://doi.org/10.1039/C9AN01584A>.

602 Molnár-Perl, I., & Horváth, K. (1997). Simultaneous quantitation of mono-, di-and trisaccharides as their TMS
603 ether oxime derivatives by GC-MS: I. In model solutions. *Chromatographia*, 45, 321- 327.
604 <https://doi.org/10.1007/BF02505578>.

605 Mucha, E., González Flórez, A. I., Marianski, M., Thomas, D. A., Hoffmann, W., Struwe, W. B., Hahm, H. S.,
606 Gewinner, S., Schöllkopf, W., Seeberger, P. H., von Helden, G., & Pagel, K. (2017). Glycan Finger-
607 printing via Cold-Ion Infrared Spectroscopy. *Angewandte Chemie International Edition*, 56,
608 11248- 11251. <https://doi.org/10.1002/anie.201702896>.

609 Nagy, G., Attah, I. K., Garimella, S. V. B., Tang, K., Ibrahim, Y. M., Baker, E. S., & Smith, R. D. (2018).
610 Unraveling the isomeric heterogeneity of glycans : Ion mobility separations in structures for lossless

611 ion manipulations. *Chemical Communication*, 54, 11701- 11704.
612 <https://doi.org/10.1039/C8CC06966B>.

613 National Research Council (US). (2012). *Committee on Assessing the Importance and Impact of Glycomics*
614 *and Glycosciences. Trans-forming Glycoscience A Roadmap for the Future*. National Academies
615 Press. https://www.ncbi.nlm.nih.gov/books/NBK109958/pdf/Bookshelf_NBK109958.pdf.

616 Nozal, M. J., Bernal, J. L., Toribio, L., Alamo, M., Diego, J. C., & Tapia, J. (2005). The Use of Carbohydrate
617 Profiles and Chemometrics in the Characterization of Natural honeys of identical geographical ori-
618 gin. *Journal of Agricultural and Food Chemistry*, 53, 3095- 3100. <https://doi.org/10.1021/jf0489724>.

619 Paglia, G., Williams, J. P., Menikarachchi, L., Thompson, J. W., Tyldesley-Worster, R., Halldórsson, S.,
620 Rolfsson, O., Moseley, A., Grant, D., Langridge, J., Palsson, B. O., & Astarita, G. (2014). Ion Mobil-
621 ity Derived Collision Cross Sections to Support Metabolomics Applications. *Analytical Chemistry*, 86,
622 3985- 3993. <https://doi.org/10.1021/ac500405x>.

623 Pu, Y., Ridgeway, M. E., Glaskin, R. S., Park, M. A., Costello, C. E., & Lin, C. (2016). Separation and Identi-
624 fication of Isomeric Glycans by Selected Accumulation-Trapped Ion Mobility Spectrometry-Electron
625 Activated Dissociation Tandem Mass Spectrometry. *Analytical Chemistry*, 88, 3440- 3443.
626 <https://doi.org/10.1021/acs.analchem.6b00041>.

627 Riggs, D. L., Hofmann, J., Hahm, H. S., Seeberger, P. H., Pagel, K., & Julian, R. R. (2018). Glycan Isomer
628 Identification Using Ultraviolet Photodissociation Initiated Radical Chemistry. *Analytical Chemistry*,
629 90, 11581- 11588. <https://doi.org/10.1021/acs.analchem.8b02958>.

630 Ruiz-Matute A.I., Brokl M., Soria A.C., Sanz M.L., Martínez-Castro I. (2010) Gas chromatographic–mass
631 spectrometric characterisation of tri- and tetrasaccharides in honey. *Food Chemistry*, 120, 637-642.
632 <https://doi.org/10.1016/j.foodchem.2009.10.050>.

633 Sanz, M.L., Polemis, N., Morales, V., Corzo, N., Drakoularakou, A., Gibson, G. R., & Rastall, R. A. (2005). In
634 Vitro Investigation into the Potential Prebiotic Activity of Honey Oligosaccharides. *Journal of Agri-
635 cultural and Food Chemistry*, 53, 2914- 2921. <https://doi.org/10.1021/jf0500684>.

636 Sanz, M.L., Sanz, J., & Martínez-Castro, I. (2004). Gas chromatographic–mass spectrometric method for the
637 qualitative and quantitative determination of disaccharides and trisaccharides in honey. *Journal of*
638 *Chromatography A*, 1059, 143- 148. <https://doi.org/10.1016/j.chroma.2004.09.095>.

639 Schindler, B., Barnes, L., Renois, G., Gray, C., Chambert, S., Fort, S., Flitsch, S., Loison, C., Allouche, A.-R.,
640 & Compagnon, I. (2017). Anomeric memory of the glycosidic bond upon fragmentation and its con-
641 sequences for carbohydrate sequencing. *Nature Communications*, 8, 973.
642 <https://doi.org/10.1038/s41467-017-01179-y>.

643 Schindler, B., Laloy-Borgna, G., Barnes, L., Allouche, A.-R., Bouju, E., Dugas, V., Demesmay, C., & Compa-
644 gnon, I. (2018). Online Separation and Identification of Isomers Using Infrared Multiple Photon Dis-
645 sociation Ion Spectroscopy Coupled to Liquid Chromatography: Application to the Analysis of Di-
646 saccharides Regio-Isomers and Monosaccharide Anomers. *Analytical Chemistry*, 90, 11741- 11745.
647 <https://doi.org/10.1021/acs.analchem.8b02801>.

648 Varki, A. (2015). *Essentials of Glycobiology* (3rd Ed., Vol. 1). Cold Spring Harbor Laboratory Press.

649 Wei, J., Wu, J., Tang, Y., Ridgeway, M. E., Park, M. A., Costello, C. E., Zaia, J., & Lin, C. (2019). Characteri-
650 zation and Quantification of Highly Sulfated Glycosaminoglycan Isomers by Gated-Trapped Ion Mo-
651 bility Spectrometry Negative Electron Transfer Dissociation MS/MS. *Analytical Chemistry*, 91,
652 2994- 3001. <https://doi.org/10.1021/acs.analchem.8b05283>.

653 Xie, C., Wu, Q., Zhang, S., Wang, C., Gao, W., Yu, J., & Tang, K. (2020). Improving glycan isomeric separa-
654 tion via metal ion incorporation for drift tube ion mobility-mass spectrometry. *Talanta*, 211, 120719.
655 <https://doi.org/10.1016/j.talanta.2020.120719>.

656 Zheng, X., Aly, N. A., Zhou, Y., Dupuis, K. T., Bilbao, A., Paurus, V. L., Orton, D. J., Wilson, R., Payne, S.
657 H., Smith, R. D., & Baker, E. S. (2017). A structural examination and collision cross section database
658 for over 500 metabolites and xenobiotics using drift tube ion mobility spectrometry. *Chemical Sci-*
659 *ence*, 8, 7724- 7736. <https://doi.org/10.1039/C7SC03464D>.

660 Zheng, X., Zhang, X., Schocker, N. S., Renslow, R. S., Orton, D. J., Khamsi, J., Ashmus, R. A., Almeida, I.
661 C., Tang, K., Costello, C. E., Smith, R. D., Michael, K., & Baker, E. S. (2017). Enhancing glycan
662 isomer separations with metal ions and positive and negative polarity ion mobility spectrometry-mass

663 spectrometry analyses. *Analytical and Bioanalytical Chemistry*, 409, 467- 476.

664 <https://doi.org/10.1007/s00216-016-9866-4>.

665